Mechanisms of Development 156 (2019) 8–19

Contents lists available at ScienceDirect

Mechanisms of Development

journal homepage: www.elsevier.com/locate/mod

Hemodynamic force is required for vascular smooth muscle cell recruitment to blood vessels during mouse embryonic development

Rachel L. Padget, Shilpa S. Mohite, Tanner G. Hoog, Blake S. Justis, Bruce E. Green, Ryan S. Udan*

Department of Biology, Missouri State University, United States of America

ARTICLE INFO

Keywords:
Mouse embryo
Vascular maturation
Vascular smooth muscle cell
Hemodynamic force

ABSTRACT

Blood vessel maturation, which is characterized by the investment of vascular smooth muscle cells (vSMCs) around developing blood vessels, begins when vessels remodel into a hierarchy of proximal arteries and proximal veins that branch into smaller distal capillaries. The ultimate result of maturation is formation of the tunica media—the middlemost layer of a vessel that is composed of vSMCs and acts to control vessel integrity and vascular tone. Though many studies have implicated the role of various signaling molecules in regulating maturation, no studies have determined a role for hemodynamic force in the regulation of maturation in the mouse. In the current study, we provide evidence that a hemodynamic force-dependent mechanism occurs in the mouse because reduced blood flow mouse embryos exhibited a diminished or absent coverage of vSMCs around vessels, and in normal-flow embryos, extent of coverage correlated to the amount of blood flow that vessels were exposed to. We also determine that the cellular mechanism of force-induced maturation was not by promoting vSMC differentiation/proliferation, but instead involved the recruitment of vSMCs away from neighboring low-flow distal capillaries towards high-flow vessels. Finally, we hypothesize that hemodynamic force may regulate expression of specific signaling molecules to control vSMC recruitment to high-flow vessels, as reduction of flow results in the misexpression of *Semaphorin 3A*, *3F*, *3G*, and the Notch target gene *Hey1*, all of which are implicated in controlling vessel maturation. This study reveals another role for hemodynamic force in regulating blood vessel development of the mouse, and opens up a new model to begin elucidating mechanotransduction pathways regulating vascular maturation.

1. Introduction

Throughout embryogenesis, developing blood vessels must undergo a highly coordinated process to produce a branched hierarchy of arteries, veins and capillaries having specific morphologies, and physical and functional characteristics. Regulation of this process is complex and is driven by molecular cues produced in the embryonic mesoderm and within the vessels themselves (Blanco and Gerhardt, 2013; Udan et al., 2013a), as well as biomechanical cues produced by blood flow—herein referred to as hemodynamic force (Culver and Dickinson, 2010; Garcia and Larina, 2014). Molecular cues of blood vessel formation, such as vascular endothelial growth factor (Vegf) or platelet-derived growth factor (Pdgf) signaling, have been known since the 1990s (Ambrus et al., 1991; Wilting et al., 1993). Ten to twenty years later, we have learned more about the role of hemodynamic force in regulating many aspects of blood vessel development, from arterial specification to blood vessel remodeling, vessel regression, and maturation (Chen et al., 2017; Chong et al., 2011; Jones et al., 2008; le Noble et al., 2003; Lucitti et al., 2007; Yashiro et al., 2007).

The use of various model organisms has been instrumental at revealing the role of hemodynamic force in blood vessel development. Studies in chicken embryos, and later in the mouse, have revealed that hemodynamic force is involved in maintaining arterial fates (Chong et al., 2011; Jones et al., 2008; le Noble et al., 2003). In mouse embryos, hemodynamic force was shown to be required to remodel yolk sac blood vessels, a process that reconstructs a capillary bed into large-diameter, proximal vessels that branch into small-diameter, distal capillaries (Lucitti et al., 2007), and these size differences correlated well to the amount of flow that the capillaries were exposed to (Udan et al., 2013b). In mouse embryos and zebrafish larvae, hemodynamic force was shown to be required for the persistence of blood vessels (sixth branch arch arteries in mice and brain vasculature in zebrafish); whereas, reduction of force in the same vessels results in their regression (Chen et al., 2012; Yashiro et al., 2007). Most recently, it was

* Corresponding author.
E-mail address: ryanudan@missouristate.edu (R.S. Udan).

https://doi.org/10.1016/j.mod.2019.02.002
Received 27 July 2018; Received in revised form 16 January 2019; Accepted 16 February 2019
Available online 21 February 2019
0925-4773/

revealed that zebrafish larvae require hemodynamic force to regulate investment or coverage of mural cells (vascular smooth muscle cells [vSMCs]) around the endothelium of developing vessels, a process referred to as vascular maturation (Chen et al., 2017). Vascular maturation is a critical aspect of blood vessel formation, as it promotes formation of the tunica media—a layer of vSMCs that contributes to the integrity of the vessel wall and is needed to control contractile tone. What remains unknown is whether hemodynamic force controls maturation in mammals.

In the present study, we reveal that hemodynamic force is required for vessel maturation in the mouse, as embryos with impaired heart contraction exhibit a diminished or absent coverage of vSMCs around extraembryonic and intraembryonic vessels. Further, we show that there are differences in the extent of vSMC coverage around various vessel subtypes, with proximal arteries having highest coverage, proximal veins having intermediate coverage, and distal capillaries having lowest coverage. This difference in coverage is similar to what has been reported in adult vessels, and correlates well to the levels of hemodynamic force exhibited in developing arteries, capillaries and veins—during stages when vSMC investment occur (Udan et al., 2013b). We also reveal the cellular mechanism for hemodynamic-force regulated coverage does not involve localized vSMC differentiation and/or proliferation around high-flow proximal vessels, but instead involves the recruitment of vSMCs from distal capillary regions to the proximal vessels. Finally, we show that reduction of flow results in an increase in *Semaphorin 3A* expression (a possible chemorepulsive molecule for vSMCs), and a decrease in *Semaphorin 3F*, and *3G* (possible chemoattractant molecules for vSMCs), as well as a downregulation in the Notch target gene *Hey1* (an important regulator of maturation). In summary, this study provides a new model to study hemodynamic-force regulated vessel maturation in mammals. This can have important implications in understanding how blood vessel walls weaken such as in segmental thinning of the umbilical cord that can lead to fetal distress, or congenital aneurysms that can affect the health of individuals from childhood to adulthood.

2. Materials and methods

2.1. Mice

Mice were on a CD1 background and contained a loss-of-function mutation in the *Myosin light chain 7* (*Myl7*) gene, also known as *Myosin regulatory light chain 2, atrial isoform* (*Mlc2a*) gene (Huang et al., 2003). *Myl7* is expressed specifically in the atria of the heart, and the normal function of Myl7 protein is to participate in contractions. Thus, experimental embryos that were homozygous mutant for the gene ($Myl7^{-/-}$: reduced-flow embryos) exhibited a reduction in blood flow throughout the embryo and yolk sac; whereas heterozygous control embryos ($Myl7^{+/-}$: normal-flow embryos) exhibited normal blood flow. To enhance fluorescence detection of the vSMCs, transgenic *Sma-myr::mCherry* mice (Armstrong et al., 2010) were used together with relevant *Myl7* genotypes. All mice were cared for using IACUC-approved animal protocols (18-018.0 and 18-019.0).

2.2. Immunostaining

For whole-mount immunostainings, embryos were dissected out of the uterus in PBS, and the whole embryo and yolk sac were kept intact. A small hole was placed at the top of the ectoplacental cone to ensure washes could properly penetrate into the yolk sac. Embryos with yolk sacs attached were then incubated in 4% paraformaldehyde (PFA) in phosphate buffered saline (PBS) for 35 min with shaking at room temperature. Samples were subsequently washed several times with PBS, followed by PBT (PBS with 0.1% Triton). Samples were blocked in blocking buffer (5% serum [Donkey or Goat, depending on antibodies being used] and 1% Bovine Serum Albumin in PBT) for 1 h at room temperature. All other antibody incubations or washes were performed at 4 °C in SBT (2.5% serum in PBT) using standard procedures. Primary antibodies used were anti-Vegfr2 (Sigma, Cat # V1014), anti-phospho Histone H3 ([PH3], Millipore, Cat#: 06-570), anti-Actin α-Smooth muscle-Cy3™ ([Sma-Cy3], Sigma, Cat# C6198). Secondary antibodies used were Donkey anti-Rabbit IgG::AlexaFluor 488 (Invitrogen, Cat # A21206), Donkey anti-Goat IgG::AlexaFluor 488 (Invitrogen, Cat # A11055). After incubating and washing, yolk sacs were removed from the embryo, flat mounted on a glass slide [arterial side oriented in the same direction], topped with Fluoromount™ (Sigma, Cat # F4680) followed by a glass coverslip. For each yolk sac, the embryo was used for genotyping using standard DNA extraction and PCR procedures.

For frozen sections, embryos were dissected and fixed as described above. The embryos were then washed in PBS and PBT, and dehydrated in a series of sucrose solutions: 15% Sucrose (1× PBS) and 30% Sucrose (1× PBS). After dehydration, the embryos were incubated in a series of solutions for a day each: a 1:1 solution of 30% Sucrose (1× PBS):Optical Cutting Temperature (OCT) solution, 1:2 30% Sucrose (1× PBS):OCT and 100% OCT. After the 2 day incubation, the embryos were embedded in 100% OCT in a plastic mold, and frozen using dry ice. Frozen blocks were then sectioned on a cryostat (Leica CM1860 UV) to produce 10 μm slices, and the sections were mounted onto silane-treated glass slides. Only half of the embryo/yolk sac was sectioned. The other half was used for genotyping. For the immunostaining, the glass slides were placed in coplin jars, and washed in PBS to remove the OCT. Sections were then post-fixed in 4% PFA in PBS for 10 min, and subsequently washed and incubated in PBS, PBT, blocking buffer and SBT using standard procedures. After the immunostaining procedure, the sections were topped with Fluoromount™ and a glass coverslip.

2.3. Imaging

Samples were imaged using an Olympus DSU IX81 spinning disk confocal microscope with a Hamamatsu ImageEM camera, and a 3i laser with 488 nm and 561 nm lasers. The following Olympus objectives were used: 40× UPlanSApo objective, 20× LUCPlanFLN (NA 0.45) objective, and 10× UPlanSApo (NA 0.4) objective. The confocal microscopy software used was SlideBook (3i). For red and green fluorescence, intensity was set to 200, camera exposure was at 50 ms, and averaging was set to eight. For general detection of staining, the camera was set to autoscale. For comparative immunostaining detection, a region of medium-high fluorescence intensity was chosen, autoscale was selected to choose the minimum and maximum intensity settings. Then, these settings were used for every image. Thus, relative fluorescence could be analyzed by comparing samples imaged at the same time, with the same settings.

2.4. Image analysis

To determine thickness of the endothelial and vSMC layers, cross-sections of dorsal aortae from normal-flow and reduced-flow embryos were analyzed. Thickness was measured in left and right dorsal aortae from several sections, and for each vessel, the thickness of the endothelium (or vSMC layer) was quantified at 10 equidistant points around the vessel. Measurements were made using the Slidebook 6 reader software.

To determine mitotic index, whole yolk sacs were immunostained with Sma-Cy3, and phospho-Histone H3 (PH3), and several 40× images were taken. Single vSMCs, that were doubly labeled with Sma-Cy3 and *Sma-myr::mCherry*, could not be detected as single cells when they were clustered together. Thus, the percent area of vSMCs occupied was assessed in every image. This was done by binarizing the vSMC signal, and quantifying the area occupied by Image J. Phospho-Histone H3 and Sma-Cy3 double positive vSMCs were easy to detect, because Sma-Cy3 is a cytosolic marker, and PH3 is a nuclear marker, so the

green staining would be found inside of a red cell with the nucleus devoid of red staining. The total number of PH3+ vSMCs was divided by the percent area occupied by vSMCs per image to derive the mitotic index. A similar strategy was used to determine the percent area occupied by vSMCs in yolk sac capillary regions, but for that analysis, there was no need to quantify mitotic cells.

2.5. Flow cytometry

To isolate single cells, a single yolk sac or embryo was placed in a microcentrifuge tube and incubated in Hank's balanced salt solution with magnesium chloride and calcium chloride ([HBSS+] Gibco™, Cat # 14025092), and 0.2% collagenase (Fisher Scientific, Cat # 17101015) in a 37 °C incubator (5% CO_2, 95% air) for 20 min. Every 4 min, the tissue was broken up further by passing through pipet tips and at the end a 25-gauge needle. The sample was then passed through a 40um cell strainer (Fisher Scientific, Cat # 22-363-547), collected in a microcentrifuge tube, centrifuged at 300*g* for 10 min, and fixed 2% PFA. Samples were then centrifuged, resuspended in Permwash (Biolegend, Cat# 421002) in 2.5% normal donkey serum (NDS), and incubated for 10 min. Then, cells were resuspended in the same solution for 15 min, with or without the antibody (anti-Sma-Cy3). Cells were centrifuged, resuspended in Permwash, and flow cytometry was performed.

A BD Accuri C6 Flow Cytometer was used, and set to analyze 1,000,000 events that included a forward side scatter over 10,000. A no antibody control was used to assess the levels of autofluorescence in the red channel, and this was used to set the gate. Only events that fluoresced at 10^4 or higher were selected.

2.6. Quantitative PCR methods

qPCR was performed on yolk sacs because they are thin tissues only comprised of endoderm and mesoderm, but with a very extensive vascular network. Thus, changes in gene expression in the yolk sac highly represent changes in gene expression in the vasculature. Two genotypes were assessed: normal flow yolk sacs (*Myl7*$^{+/-}$, heterozygous), and reduced-flow yolk sacs (*Myl7*$^{-/-}$, homozygous). For each yolk sac, RNA was extracted and purified using an RNeasy kit (Qiagen, catalog #: 74104) with the on-column DNase digestion step (Qiagen, catalog # 79254). RNA concentrations (and later cDNA concentrations) were verified using the Qubit fluorometer and reagents (Company, catalog #: Q10210 and catalog #: Q10212), and cDNA was synthesized using the GoScript™ Reverse Transcriptase system (Promega, catalog #: A5000). Three to four yolk sacs were isolated for each group (groups: *Myl7*$^{+/-}$ and *Myl7*$^{-/-}$), and two technical replicates were ran for each yolk sac sample. For the qPCR reaction, the GoTaq® qPCR master mix was used (Promega, catalog #: A6001), and the samples were run on a MX3005P qPCR thermocycler (Stratagene, catalog #: MX3005P) under the following conditions: 95 °C 10 min, 40 cycles of 95 °C 30 s; 56 °C 30 s; 72 °C 30 s, 1 cycle of 95 °C 1 min; 60 °C 1 min; 95 °C 30 s. Ct values were taken by automatic thresholding, and the change in gene expression was determined using the $2^{-\Delta\Delta Ct}$ method (Livak and Schmittgen, 2001). For each qPCR reaction, the mean normalized expression of each sample was determined for both the reference/housekeeping gene and the gene-of-interest, and a student's *t*-test was used to determine if there was a significant difference in gene expression between the reduced-flow versus normal-flow yolk sacs. Results were verified for select genes using new sets of yolk sacs.

A variety of qPCR target genes were evaluated. For reference/housekeeping genes, GAPDH was primarily used, though Rpl13a was used on occasion to verify gene expression differences detected with GAPDH, and similar results were obtained (data not shown). For vSMC differentiation, five well-established target genes were chosen (Table 1). To assess vSMC recruitment, 18 candidate target genes were chosen based on previous literature implicating their roles in vSMC recruitment (Table 1). All sequences to the forward and reverse primers are provided in Table 1.

Table 1
List of primers used for qPCR of housekeeping/reference genes, vSMC differentiation genes, vSMC marker genes, and vSMC recruitment genes.

Name of gene	Forward primer (5′-3′)	Reverse Primer (5′-3′)
Acta2/Sma	TCCCTGGAGAAGAGCTACGA	ATAGGTGGTTTCGTGGATGC
Angpt1	CAGCACGAAGGATGCTGATA	TTAGATTGGAAGGGCCACAG
Dll1	GGTGTGATGACCAACATGGA	GACAACCTGGGTATCGGATG
Dll4	GTGTACCAGCAACCCGTGTG	GTCTCCCCCACGAGCTTA
Efnb2	TCCCTTTGTGAAGCCAAATC	AATAAGGCCACTTCGGAACC
EphB4	AAGATGGTCAATGGGCTGAG	CCTATTTGGGGCTTGAAGGT
FoxC1	AAGACGGAGAACGGTACGTG	CTCTCGATTTTGGGCACTGT
FoxC2	GCCACCTCCTGGTATCTGAA	AAAGTTTGCTGTTGGGTTGC
Gapdh	AAATGGTGAAGGTCGGTGTG	AATCTCCACTTTGCCACTGC
Hey1	CACCTGAAAATGCTGCACAC	ACCCCAAACTCCGATAGTCC
Hey2	TGAAGATGCTCCAGGCTACA	CACTCTCGGAATCCAATGCT
Jag1	TTCAAAGTGTGCCTCAAGGA	TCCACCAGCAAAGTGTAGGA
Jag2	CCTGCTGCTTTGTGATCGAG	TCTGGATCAGGCTGCTGTC
Mkl1/Mrtf-a	GAGCAGAGAAGAAGCCTGGA	CAGAATGTGCATCCTGACCA
Mkl2/Mrtf-b	ATCCTACCTGCACCCATCAA	GCTGCTGCTGTTCTTGTCAG
Myocardin	GCATTTCTGGACAAACTGGTG	CGGATTCGAAGCTGTTGTCT
Ntn1	AGGAGGGCTTCTACCGAGAC	CAGTGGTTTGATTGCAGGTC
Pdgf-A	CAACCTGAACCCAGACCATC	CACGGAGGAGAACAAAGACC
Pdgf-B	GATCTCTCGGAACCTCATCG	GGCTTCTTTCGCACAATCTC
Pdk2	GCCAAGCTGAAGAGACGAGA	CATCTGCTCCCTGTGGATCT
Rpl13a	CTTGTGCGATGGGACTTAGC	CAAAACTGTCCCAAACAGCA
Sema3A	GGTCCTCATGCTCACGCTAT	CATGGTGCTGCAAGTCAGA
Sema3F	TGCCCTTCTCAGGAAAGATG	GATGAGTGCGCATGAAGTTG
Sema3G	AGCACAACAGCACCTTCCTT	CCGTCTGCACAACTCTCTCA
Sm22a	CAACAAGGGTCCATCCTACG	ATTGAGCCACCTGTTCCATC

2.7. Statistics

For all experiments multiple embryos were used per group were used, and several sections or images were used for each analysis. In the PH3 analysis, at least 4 embryos per group were used, and approximately 10 images per embryo were quantified. In qRT-PCR studies, 4–6 embryos per group were used. In flow cytometry, 5 embryos per group were used. In the distal capillary analysis of vSMCs, at least 4 embryos per group were used. For the tissue thickness assessment, a 2 embryos per group was used. For statistical comparisons, standard *t*-tests were performed, and standard error was used for all of the bar graphs.

3. Results

3.1.1. Maturing vessels exhibit a progressively decreased amount of vSMC coverage around proximal arteries, proximal veins and distal capillaries

One of the first locations where blood vessel maturation appears is in the earliest developing vascular bed of the embryo—the yolk sac. Emergence of vSMCs in the yolk sac begins at embryonic day (E9.5), coinciding with the formation of remodeled blood vessels. To visualize the vSMCs, two techniques could be used: 1) immunostaining with the anti-Actin smooth muscle α (Sma) antibody, or 2) use of the transgenic *Sma-myr::mCherry* fluorescent protein reporter. Using either approach alone allowed us to visualize that the large proximal vessels (i.e. vessels located closer to the heart that have higher blood flow) were covered by vSMCs (data not shown). However, in other vessels, it was very difficult to visualize thin vSMC layers and single vSMCs by themselves because the fluorescent signal was very weak in individual cells. Since we were interested in visualizing both vSMC layers as well as individual vSMCs, we combined the use of both approaches throughout the study, as this significantly enhanced contrast of the fluorescent signal. We were confident that the combined approach was appropriate to use because it had been previously shown *Sma-myr::mCherry* expression was

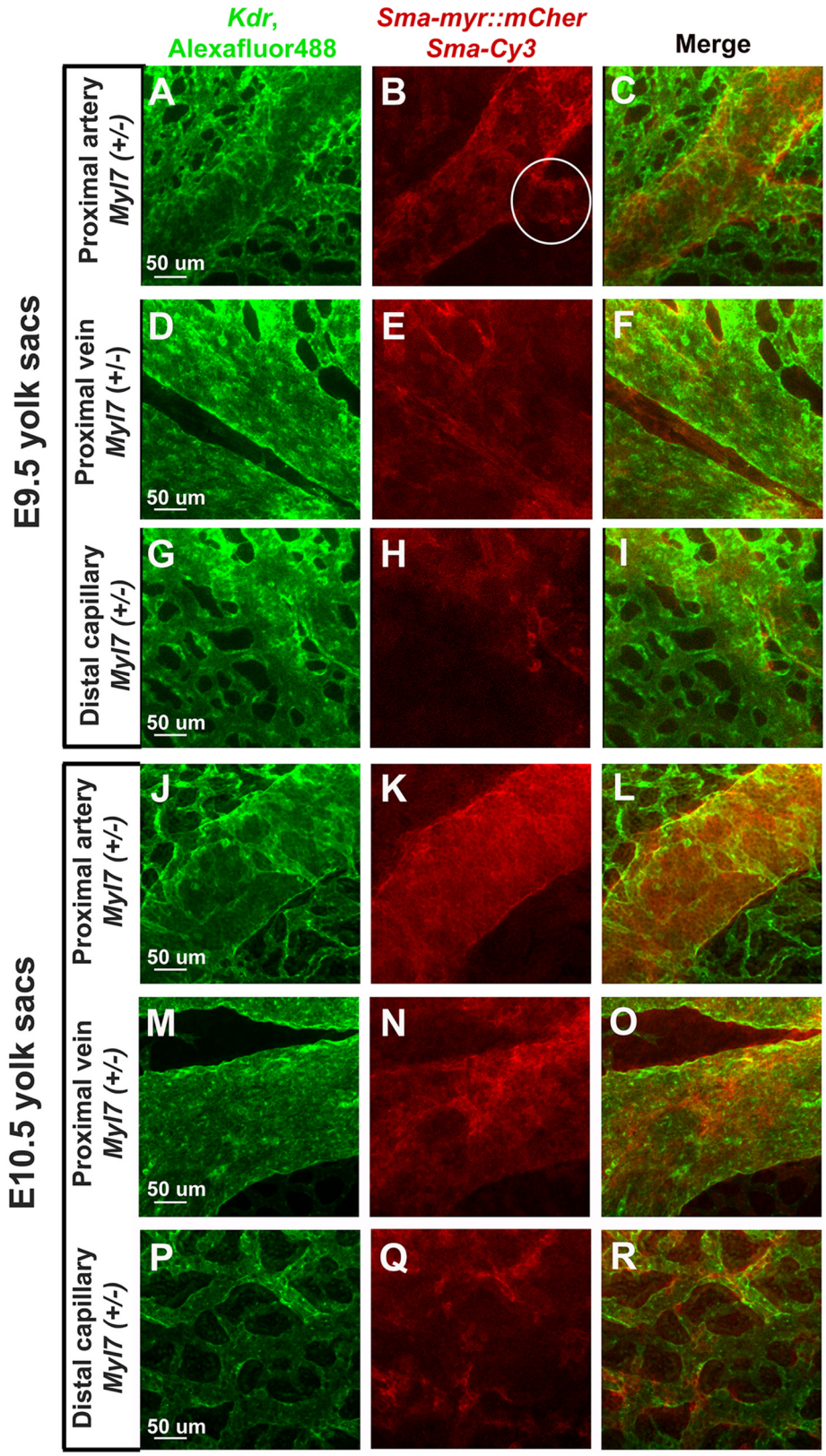

Fig. 1. Composition of vSMCs in E9.5 (A–I) and E10.5 (J–R) yolk sacs. E9.5 and E10.5 yolk sac vessels labeled with Vegfr2/AlexaFluor488 to detect the endothelium and doubly labeled for *Sma-myr::mCherry* and Sma-Cy3. E9.5 proximal arteries (A–C), proximal veins (D–F), and distal capillaries (G–I). E10.5 proximal arteries (J–L), proximal veins (M–O), and distal capillaries (P–R). For all yolk sacs, normal flow embryos were used, with a heterozygous Myl7 genotype. Scale bar is 50 μm.

coincident with Sma antibody staining (Armstrong et al., 2010).

At E9.5, confocal imaging of the doubly-labeled vSMCs revealed investment of select yolk sac blood vessels with vSMCs (Fig. 1A–I). This was most noticeable in the larger, proximal vessels. However, we were able to detect some distal yolk sac vessels with coverage, albeit at slightly lower fluorescence levels (Fig. 1B, circle). Vessels with a

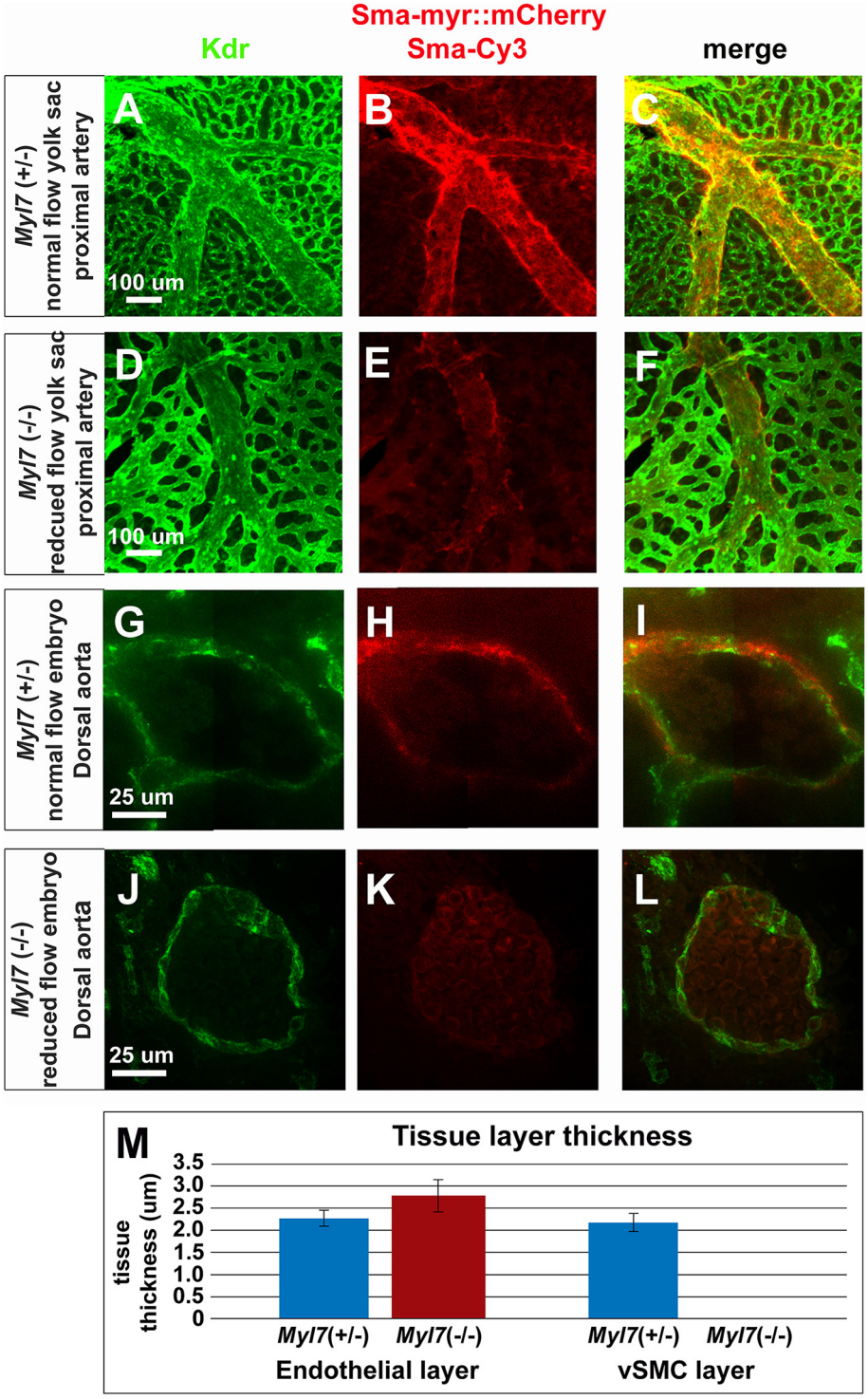

Fig. 2. Comparison of vSMC coverage in proximal yolk sac arteries (A–F) and dorsal aortae (G–L) of E10.5 normal-flow (*Myl7*$^{+/-}$) and reduced-flow (*Myl7*$^{-/-}$) embryos. Tissues were labeled with Vegfr2/AlexaFluor488 (to detect endothelial cells), and doubly labeled with *Sma-myr::mCherry* and Sma-Cy3 (to detect vSMCs). Whole-mount images were taken to detect the E10.5 normal-flow proximal arteries (A–C) and the reduced-flow proximal arteries (D–F). Cross-sections were taken to detect the E10.5 normal-flow dorsal aorta (G–I) and reduced-flow dorsal aorta (J–L). Scale bar is 100 µm. Thickness of the endothelial layer, and the vSMC layer, was quantified in dorsal aortae of normal-flow versus reduced-flow embryos.

lowered amount of coverage tended to be those that were directly connected to the proximal vessels, and presumably were exposed directly to blood flow. Alternatively, distal yolk sac vessels that were not directly connected to the proximal vessels tended to not be covered with vSMCs. If vSMCs were not covering a vessel, they would be found scattered in the yolk sac mesoderm as individual cells, typically exhibiting a spindly shape. By E10.5, more vSMCs were apparent, and maturing vessels appeared brighter (Fig. 1J–R). Similar to E9.5, E10.5 yolk sacs exhibited vSMCs that mainly surrounded the proximal vessels, but were also still found associated with other vessels or as unattached cells.

Of significant note were the differences in vSMC coverage around the different vessel subtypes. For instance, E9.5 proximal arteries (Fig. 1A–C) exhibited a greater amount of vSMC coverage than in proximal veins (Fig. 1D–F) and distal capillaries (Fig. 1G–I), though coverage in all of the vessels appeared to be mottled (Fig. 1A–C). By E10.5, proximal artery coverage became denser, as the vSMC layer did not appear mottled (Fig. 1J–L). E9.5 and E10.5 proximal veins also exhibited vSMC coverage (Fig. 1D–F, M–O), but the intensity of fluorescence was weaker than the proximal arteries, and coverage appeared mottled at both stages (Fig. 1D–F, M–O). Finally, E9.5 and E10.5 distal capillaries exhibited a reduced coverage that was sparse, and

sometimes devoid of vSMCs covering vessels (Fig. 1C). These observations support previous findings in adult vessels where thickness of the tunica media (vSMC layer of the vessel) is greater in arteries versus veins and capillaries (Isayama et al., 2013). Further, it was clear that these differences in the extent of vSMC coverage quickly become established during early vascular development.

3.2. Hemodynamic force is required for vSMC coverage during early maturation of developing vessels

Development of the yolk sac vessels themselves is highly influenced by hemodynamic forces provided by blood flow. Previous studies have shown that hemodynamic force is required for remodeling of the mouse yolk sac vessels (Lucitti et al., 2007), and the extent of hemodynamic force (or amount of blood velocities), in the E8.5 to E9.5 yolk sac vessels, correlates to differences in vessel size (Udan et al., 2013b). Thus, even before remodeling occurs (E8.5), high blood velocities are found in developing proximal arteries, medium blood velocities are found in developing proximal veins, and low blood velocities are found in developing capillaries of the yolk sac. Because the amount of hemodynamic force in these different vascular regions of the yolk sac correlates well to the extent of vascular maturation that we observed, the requirement of hemodynamic force to control vascular maturation was assessed.

To determine whether hemodynamic force is required for vascular maturation, we compared the extent of vSMC coverage in blood vessels having normal blood with those having reduced blood flow. To alter blood flow, we used a mutant mouse model that has a null mutation in the *Myl7* (*Mlc2a*) gene (Huang et al., 2003). This gene encodes a myosin motor protein that controls cardiac muscle contraction, and is expressed specifically in the atria of the heart, and its expression is not detectable in other cells (including the vasculature) throughout the E9.5-E13.5 embryo (Cai et al., 2003; Ruiz-Lozano et al., 1998). On average, homozygous mutants ($Myl7^{-/-}$) are embryonic lethal around E11.0 (as late as E11.5) (Huang et al., 2003). Directly before this time point, mutant hearts (as well as yolk sac tissues) do not exhibit signs of tissue breakdown or apoptosis. Also, they continue contracting their ventricles, but they lack atrial contractions (Huang et al., 2003). As a result, blood flow is very weak; thus, these embryos are called reduced-flow embryos. We compared extent of vSMC coverage in reduced-flow embryos to normal-flow embryos ($Myl7^{+/-}$).

In $Myl7^{-/-}$ mutant E10.5 yolk sacs, proximal arteries exhibited diminished remodeling [based on size of the vessel, previously documented in (Udan et al., 2013b)], and we also observed a decrease in the amount of vSMCs covering the arteries (as visualized by a diminished fluorescence), as compared to normal-flow ($Myl7^{+/-}$) proximal arteries (Fig. 2A–F). This decrease in vSMC coverage was also observed when comparing proximal veins between reduced-flow and normal-flow yolk sacs (Supplemental Fig. 1). These results reveal that hemodynamic force is required for normal vascular maturation.

To determine if the effect of reduced hemodynamic force was specific to yolk sac vessels, we also assessed the extent of vSMC coverage around intraembryonic vessels. To assess the most prominent vessel of the embryo (the dorsal aorta), whole-mount immunostainings were not performed, as the tissue is too thick to visualize by confocal microscopy. Thus, we decided to image cross-sections. In cross-sections of reduced-flow ($Myl7^{-/-}$) embryos, we observed that the endothelium of the dorsal aorta was a single-cell layer averaging 2.8 um in thickness, but completely devoid of a surrounding layer of vSMCs (0 μm vSMC thickness) (Fig. 2J–M). In normal-flow embryos, the dorsal aorta exhibited a similarly thin endothelium averaging 2.3 μm in thickness (no significant difference to reduced-flow embryos); however, in these embryos, vSMCs surrounded the dorsal aortae in a single-cell layer that averaged 2.2 μm in thickness (Fig. 2G–I, M). Interestingly, the impaired maturation of the dorsal aorta appears independent of an effect of remodeling, as the reduced-flow dorsal aorta was only slightly smaller in diameter than the normal-flow dorsal aorta. These results reveal that hemodynamic force is required for maturation of developing blood vessels.

3.3. Hemodynamic force does not promote localized vSMC proliferation or differentiation around developing high-flow vessels

During maturation, high-flow vessels (proximal yolk sac vessels and dorsal aortae) eventually acquire a greater amount of vSMCs than low-flow vessels (distal capillaries). Based on zebrafish studies (Ando et al., 2016; Chen et al., 2017), it may be assumed that high-flow vessels increase vSMC coverage by a migratory/recruitment mechanism; however, no studies in the mouse have directly assessed this, and there could be a different explanation for hemodynamic force-induced vSMC coverage. Thus, we propose two hypotheses for how vSMCs specifically cover high-flow proximal vessels: 1) high-flow vessels promote the localized proliferation/differentiation of vSMCs from the surrounding mesoderm, followed by a direct attachment of vSMCs around the high-flow vessels, or 2) high-flow vessels promote the recruitment/migration of vSMCs from the surrounding mesoderm.

In the first hypothesis, vessels exposed to high flow promote the localized production of vSMCs (either by promoting proliferation or differentiation), followed by the direct attachment of vSMCs to those vessels. To test if proliferation was altered by hemodynamic force, we compared the proliferative potential of vSMCs found in normal-flow versus reduced-flow yolk sacs. This was done by immunostaining entire yolks sacs with phospho-Histone H3 (a mitotic marker) and Sma-Cy3 (co-labeled with *Sma-myr::mCherry*), and counting the total number of mitotic vSMCs (phospho-Histone H3, Sma double positive cells) divided by the surface area occupied by Sma staining to derive the mitotic index. Dividing by the surface area was necessary, as some Sma + cells would overlap, appearing as one cell—making it difficult to distinguish vSMCs as single cells. Comparing the mitotic indexes revealed that there was no significant difference in the amount of vSMC division that occurs between the normal-flow and reduced flow yolk sacs (Fig. 3A–I).

Though there was no evidence that hemodynamic force affects the proliferative status of vSMCs, it is possible that it promotes the localized differentiation of vSMCs to produce more of them in regions of high-flow. vSMC differentiation can be quite complex, as it seems to be controlled by gene regulation of various transcriptional co-activators (Myocardin, Mrtf-a, and Mrtf-b), which ultimate regulate the expression of smooth muscle markers (Sm22a/Tagln, and Acta2) (Mack, 2011). To determine whether hemodynamic force promotes the differentiation of vSMCs, we assessed for global changes of vSMC differentiation markers throughout the yolk sac by isolating RNA from entire reduced-flow and normal-flow yolk sacs, and performing qRT-PCR to compare expression of differentiation targets. We expected that a reduction of flow would result in a decrease in vSMC differentiation, and thus a decrease in target gene expression. We first assessed the three coactivators. To our surprise, we observed an opposite effect—reduced-flow yolk sacs exhibited a significant increase in expression of *Myocardin* (2.2×), and *Mrtf-a* (2.0×), and a slight but significant increase in *Mrtf-b* (1.4×) (Fig. 3J). This suggests that perhaps reduction of blood flow promotes the differentiation of vSMCs, a view that is contrary to diminished vSMC coverage present in reduced-flow yolk sacs. Though vSMC coactivator expression increased, this may not have translated to an actual increase in the amount of vSMCs, as we observed no significant difference in smooth muscle markers: *Sm22a* (1×), and *Acta2* (1×) (Fig. 3J). Thus, it is likely that alterations in flow do not affect the differentiation status of vSMCs.

3.4. Hemodynamic force does not affect the total number of vSMCs present in the yolk sac

Though the evidence suggests that hemodynamic force does not alter the proliferative or differentiation status of the vSMCs, the slight

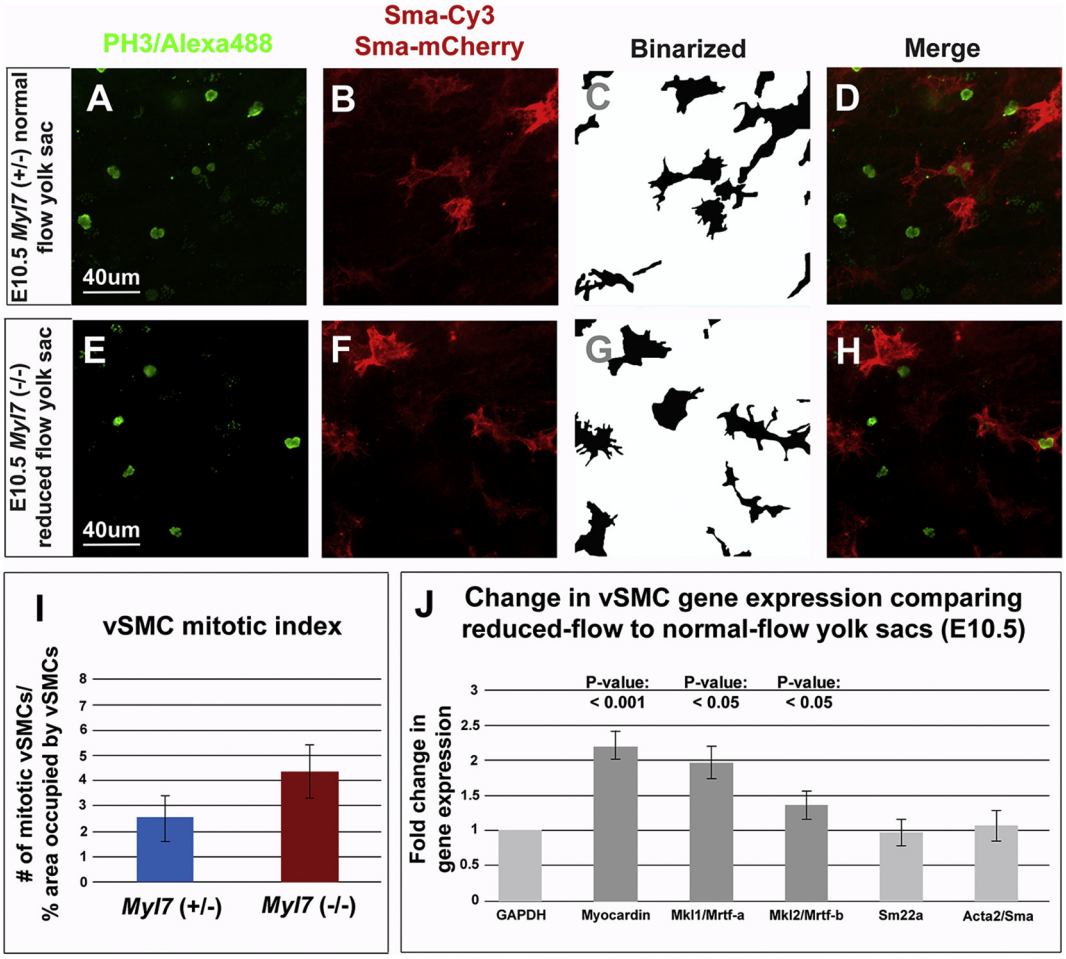

Fig. 3. Assessment of mitotic index (A–I) and vSMC differentiation (J) in reduced-flow and normal-flow yolk sac tissue. Representative whole-mount images of PH3-labled nuclei costained to detect vSMCs in normal-flow yolk sacs (A–D) and reduced-flow yolk sacs (E–H). To percent area occupied by vSMCs, Sma-positive cells were manually traced, and the image was binarized (C–G) and later quantified by Image J. To determine the mitotic index, PH3-positive vSMCs were counted in each image, and divided by the percent area occupied in that image. Approximately ten images were used per each embryo, with at least an n of 4 embryos were used per group resulting in an average 0.3 mitotic vSMCs per image (or 10 total mitotic cells per image). Scale bar is 40 um. This data is displayed graphically (I). For gene expression analysis, RNA was collected from whole normal-flow (*Myl7*$^{+/-}$) and reduced-flow (*Myl7*$^{-/-}$) yolk sacs, and qRT-PCR was performed on several vSMC differentiation or marker genes: Myocardin, Mkl1, Mkl2, Sm22a, and Sma (J). For the mitotic index, four embryos were used per each group, and a total of 10 images for each yolk sac. A student's *t*-test was performed for the ratios collected from each image, and no significant difference was determined (P = 0.59). For qPCR, a minimum of 3 embryos was used for each group, and two technical replicates were performed for each sample. For statistical analysis, a student's *t*-test was performed against the mean normalized expressions between control and mutant samples.

increase vSMC transcriptional co-activator expression led us to question whether vSMC numbers were actually impacted by flow. To settle this debate, we performed flow cytometry to compare the total number of vSMCs present in normal-flow vs. reduced-flow yolk sacs. To ensure an accurate comparison of the tissues are made [due to size differences of the reduced-flow and normal-flow yolk sacs (Udan et al., 2013b)], we specifically analyzed the ratio of Sma + cells divided by total amount of cells from normal-flow and reduced-flow whole yolk sacs. The number of Sma + cells was normalized to total amount of cells because yolk sacs exposed to a lower amount of hemodynamic force tend to be slightly smaller in size (Lucitti et al., 2007). The results revealed no significant difference in the ratio of Sma + /total cells between normal-flow and reduced-flow yolk sacs (Fig. 4A). We also performed the same study, but using tissue isolated specifically from the embryo proper, where intraembryonic vessels reside. In that assay, we also revealed no significant difference in the ratio of Sma + cells between the reduced-flow and normal-flow embryos (Fig. 4B). Thus, hemodynamic force does not influence the amount of vSMCs available, both extra-embryonically and intraembryonically.

3.5. Hemodynamic force affects recruitment of vSMCs from distal capillaries to high-flow arteries

Considering that hemodynamic force does not impact the proliferative or differentiation status of vSMCs, we next sought to determine if hemodynamic force promotes vSMC recruitment or migration. In this model, vessels exposed to high-hemodynamic force may promote recruitment of vSMCs from neighboring vessel regions to high-flow vessels. To determine whether vessels-exposed to high hemodynamic force promote the recruitment of vSMCs, we turned to confocal imaging. Though it would be ideal to visualize the migratory behaviors of the vSMCs in normal-flow versus reduced-flow embryos, this was not possible to do. For one, the transgenic line for visualizing these embryos (*Sma-myr::mCherry*) exhibits low expression; thus, use of high laser power or long exposure times leads to photodamage of the tissue. Second, the *Sma-myr::mcherry* signal only starts to emerge at E9.5, so we cannot image any investment that may occur between E8.5 to E9.5. Third, static culturing at E9.5 to E10.5 is not possible. Thus, we were not able to live image the recruitment process, and instead we assessed the recruitment process using static images.

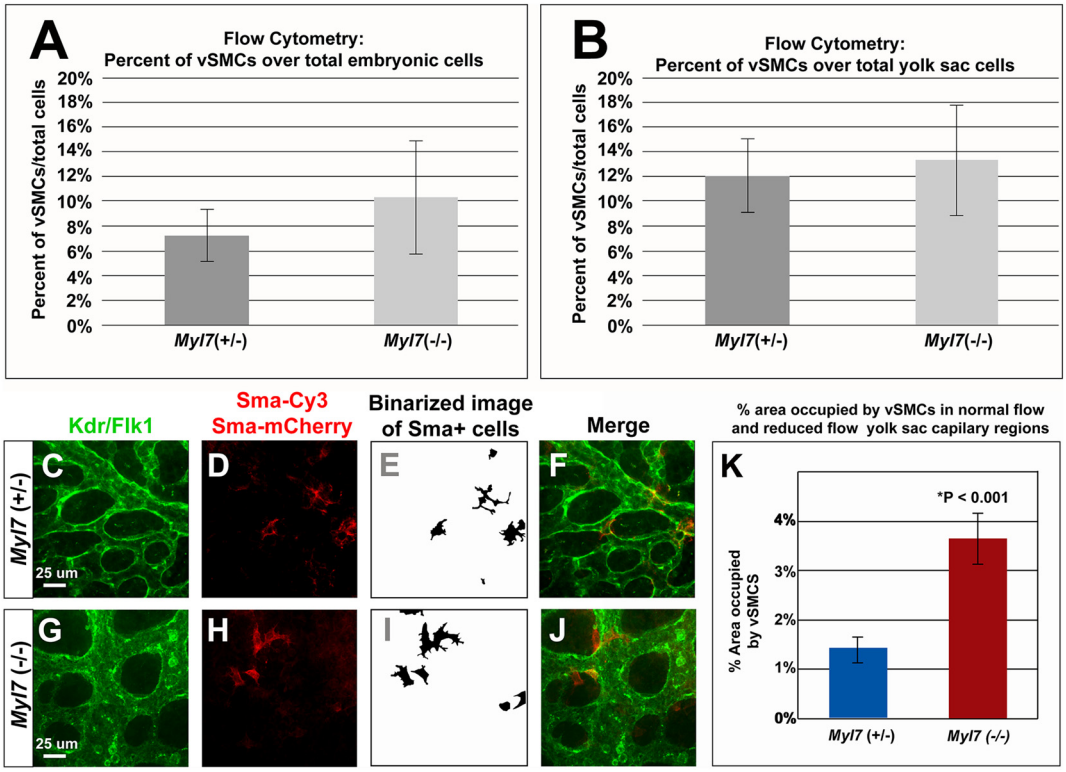

Fig. 4. Determination of the percentage of vSMCs over total yolk sac (A) or embryonic (B) cells in normal-flow and reduced-flow tissues, and assessment of percent area occupied by vSMCs in distal capillary yolk sac tissue (C–K). Whole yolk sac tissue (A) and whole embryonic tissues (B) from normal-flow embryos and reduced-flow embryos were extracted, collagenase-treated, immunostained with Sma-Cy3, and analyzed by flow cytometry to compare the relative percentage of vSMCs. 8 embryos/yolk sacs were used for each group (*Myl7*$^{+/-}$ or *Myl7*$^{-/-}$). To determine the percent of vSMCs occupied in distal capillary regions, whole-mount yolk sacs from normal-flow and reduced-flow embryos were imaged in the distal capillary regions, and labeled vSMCs (D and H) were binarized (E–F), and quantified by Image J. The percent area occupied by vSMCs in distal capillary regions was graphically displayed (K). Ten images were used for each yolk sac, and an n of at least 4 embryos were used per group. Scale bar is 25 μm. For flow cytometry experiments and vSMC analysis in capillary regions, a student's *t*-test was performed to determine statistical significance.

Our rationale for deducing migratory behaviors from static images depends on the whether there are differences in the amount of vSMCs found in proximal versus distal regions of the yolk sac. Specifically, we posited that normal-flow yolk sacs exhibit a bias of vSMCs in proximal vessel regions as compared to distal capillary regions. This is based on the hypothesis that proximal vessels exposed to high hemodynamic force recruit vSMCs from distal regions. This is analogous to the movement of endothelial cells from distal-capillaries to proximal-arteries (Udan et al., 2013b), but instead single vSMCs would migrate in the mesoderm towards the proximal vessels. Thus, in reduced-flow yolk sacs, we anticipate more vSMCs found in distal capillaries, as the recruitment signal towards the proximal vessels would be lacking. We compared the amount of vSMCs found (percent area occupied by vSMCs) in distal capillary regions between normal-flow and reduced-flow yolk sacs, and determined a significantly higher amount of vSMCs in the reduced-flow distal capillary regions (Fig. 4C–K). Considering that normal-flow and reduced-flow yolk sacs retain the same amount of total vSMCs, this result reveals that vSMCs in distal capillaries must be migrating away from distal capillary regions to proximal vessel regions.

3.6. Hemodynamic force may regulate Semaphorin 3 molecules and Notch signaling to control vSMC recruitment/coverage

To determine the mechanism for how hemodynamic force promotes maturation of high-flow vessels, we compared expression of candidate genes known to regulate vSMC coverage in reduced-flow versus normal-flow yolk sacs using qPCR. Various studies have elucidated a host of candidate genes known to regulate vSMC coverage, and many of these genes encode paracrine ligands that participate in communication between endothelial and mural cells (Finney and Orr, 2018). For example, vSMC-secreted Angiopoietin1 (Angpt1) helps to stabilize vSMC-endothelial interactions by promoting endothelial expression of unidentified growth factors which enhance recruitment and/or proliferation of the vSMCs (Dewachter et al., 2006; Folkman and D'Amore, 1996; Suri et al., 1996; Vikkula et al., 1996). Pdgfs (such as Pdgf-B or Pdgf-A), which are expressed in endothelial cells, exhibit mitogenic and chemoattractant properties promoting the proliferation and/or recruitment of vSMCs from surrounding tissues (French et al., 2008; Grotendorst et al., 1982; Hellström et al., 1999; Jawien et al., 1992; Lindahl et al., 1997; Ross et al., 1974). Though primarily known as neural guidance molecules, Netrins (such as Netrin 1 [Ntn1]) also have a proposed role in mural cell investment, as Ntn1 has been shown to have a chemoattractant effect on vSMCs in vitro (van Gils et al., 2012). Though these are interesting candidates, upon comparing expression of these genes (*Angpt1*, *Pdgf-A*, *Pdgf-B*, *Ntn1*) between reduced-flow versus normal-flow yolk sacs, we found no significant difference (Fig. 5A).

Though we failed to find a change in gene expression for *Angpt1*, *Pdgf-A*, *Pdgf-B*, or *Ntn1*, we did observe gene expression differences in other candidates, such as *Semaphorins*, that also regulate maturation and participate in paracrine signaling. Though Semaphorins have traditionally been thought of as guidance molecules that act to repel or attract axonal growth cones by signaling to neurons via varied receptors (Plexins, Nrp1-2, and Vegfr2), a role has been attributed to the regulation of vSMC coverage (Epstein et al., 2015; Gu and Giraudo, 2013). For example, blocking Semaphorin 3A's (Sema3A) ability to interact with the Nrp1 receptor resulted in an increase in vSMC coverage of lymphatic vessels of the mouse adult intestine—suggesting a chemorepulsive role for Sema3A (Jurisic et al., 2012). On the other hand,

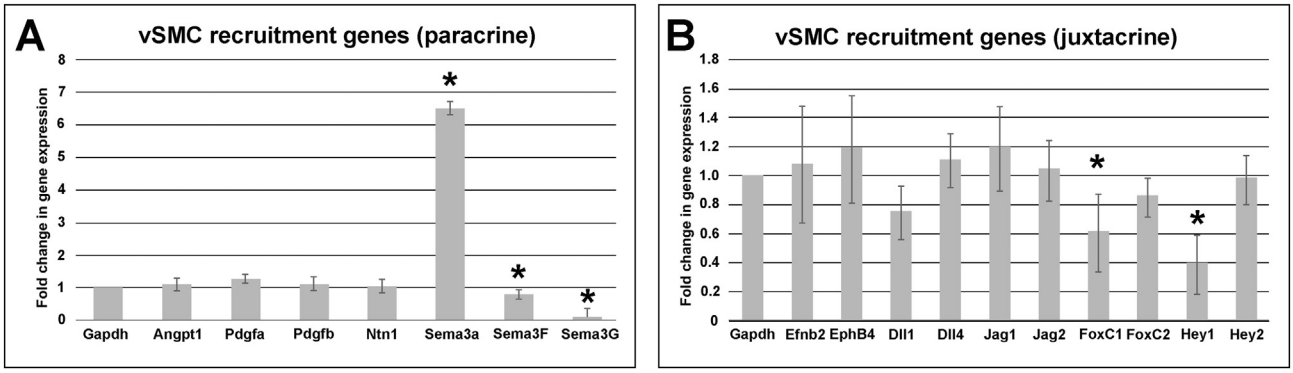

Fig. 5. Relative gene expression analysis of vSMC recruitment genes in reduced-flow yolk sacs compared to normal-flow yolk sacs. qPCR of reduced-flow yolk sac samples as compared to normal-flow yolk sac samples to assess expression differences for paracrine genes (A), or juxtacrine/juxtacrine-related genes (B), known to control vascular maturation. Genes with a significant difference had a P-value < 0.05 (*) according to a *t*-test of mean normalized expression for each group (see material and methods). A minimum of 3 yolk sacs were taken per group, with two technical replicates for each yolk sac/gene.

Semaphorin 3F (Sema 3F) may have chemoattractant properties, as its expression increases vSMC coverage in an adult tumor mouse model (Wong et al., 2012). Similarly, endothelial-expressed Semphorin 3G (Sema 3G) can promote vSMC migration in vitro (Kutschera et al., 2011). Analysis of *Sema3A*, *Sema3F*, and *Sema3G* expression in the reduced-flow versus normal-flow yolk sacs revealed an interesting result. *Sema3A* exhibited a 6.5× increase in expression, *Sema3F* exhibited a slight but significant decrease (0.8×), and *Sema3G* exhibited a significant decrease (0.1×) in expression in the reduced-flow yolk sacs (Fig. 5A). Considering the potential chemorepulsive and chemoattractant actions of these molecules, we propose that hemodynamic force may regulate expression of these Semaphorins to regulate vSMC recruitment, either by downregulating chemorepulsive Semaphorin 3 molecules or upregulating chemoattractant Semaphorin 3 molecules.

Secreted ligands, such as Semaphorin 3 molecules or other chemoattractant/chemorepulsive molecules, may explain how vSMCs could be recruited several cell distances away from high-flow vessels within the yolk sac. However, activation of cell migration, though important for recruitment, may be counterproductive when it comes to commencing cell adhesion, and coverage around vessels. Thus, one hypothesis to explain vSMC investment is a two-step process: 1) hemodynamic force promotes the endothelial expression of secreted molecules that control vSMC recruitment, and 2) hemodynamic force promotes the endothelial expression of membrane-bound ligands that, upon contact with a vSMC, promotes adhesion.

To address the second step, we assessed expression of candidate genes that participate in juxtacrine signaling, but also have roles in vessel maturation. For example, *EphrinB2* and *EphB4* are very well characterized genes exhibiting arterial endothelial cell and venous endothelial cell expressions, respectively (Wang et al., 1998). However, they are also expressed in mural cells, and through reciprocal signaling between endothelial and mural cells, they help to stabilize vSMC-endothelial interactions by reducing mural cell motility and promoting focal adhesion formation (Foo et al., 2006; Gale et al., 2001; Korff et al., 2008; Shin et al., 2001). In our study, analysis of *EphrinB2* and *EphB4* revealed no significant difference between reduced-flow and normal-flow yolk sacs (Fig. 5B). Also, many studies have shown that Notch is required for vSMC coverage (Doi et al., 2006; Domenga et al., 2004; High et al., 2008), and several pieces of evidence suggest that Notch signaling members are flow responsive in endothelial cells (Chen et al., 2017; Jahnsen et al., 2015; Masumura et al., 2009; Obi et al., 2009). Upon analyzing expression of Notch ligands, we observed no significant difference in expression of *Dll1*, *Dll4*, *Jag1* and *Jag2* in reduced-flow versus normal-flow yolk sacs (Fig. 5B). However, we did observe a significant decrease in expression of the Notch target gene *Hey1* (0.4×), suggesting that Notch activity may be modulated by flow independently of Notch ligands (Fig. 5B). Considering that FoxC2 has been shown to physically and functionally interact with Notch to promote expression of another Notch target gene (*Hey2*) in endothelial cells (Hayashi and Kume, 2008), and the zebrafish homologs to FoxC1 and FoxC2 are both flow responsive and both required for vascular smooth muscle cell coverage (Chen et al., 2017), we decided to assess *FoxC1* and *FoxC2* levels in the reduced-flow yolk sacs. *FoxC2* levels did trend towards a decrease, but it was not significantly different (Fig. 5B). However, we did observe a significant downregulation (0.6×) of *FoxC1* (Fig. 5B). Taken together, these data suggest that Notch signaling may be modulated in response to flow. Though, a mechanism for this downregulation is unknown at this time.

4. Discussion

In this study, we determined that hemodynamic force promotes blood vessel maturation during mouse embryonic development. This was based on the main observation that reduction of blood flow resulted in diminished/absent vSMC coverage around both intraembryonic (dorsal aorta) and extraembryonic (yolk sac) vessels. It is possible that the amount of hemodynamic force that blood vessels are exposed to determines the amount of vSMC coverage, as vSMC coverage was greater in arteries, than in veins and capillaries. This correlates well with the amount of blood flow exhibited in the different vessel subtypes, with the highest blood flow present in the developing proximal arteries (Udan et al., 2013b). We also show that the cellular mechanism of vSMC coverage involves the migration of vSMCs in the mesoderm from low-flow distal capillary regions to high-flow vessels, instead of localized vSMC differentiation/proliferation mechanism that would occur around the high-flow vessels. Finally, we reveal a potential molecular mechanism whereby hemodynamic force promotes (or inhibits) the expression of chemoattractive Sema3 molecules (or inhibits expression of chemorepulsive Sema3 molecules) to regulate recruitment of vSMCs throughout the yolk sac to high-flow vessels, followed by the upregulation of the Notch target gene *Hey1*, presumably to enhance the adhesion of the vSMCs once they reach the high-flow vessels.

Hemodynamic-force regulated maturation seems to be a conserved process from mammals to fish. In Chen et al., reduction of hemodynamic force in zebrafish embryos, via depletion of blood cells in *gata1* morphants or impairment of heart contraction in *tnnt2* morphants, results in a marked reduction in the number of mural cells present around vessels (Chen et al., 2017). Also in zebrafish, mural cell coverage likely occurs via a recruitment process, and not a differentiation mechanism, as live imaging studies have revealed that loss of blood flow does not prevent the emergence of mural cells, but does block their recruitment to vessels (Ando et al., 2016). These studies correlate well with our findings in mice.

Though hemodynamic-force regulated maturation may be

evolutionarily conserved, the exact mechanotransduction mechanisms regulating maturation may be multifactorial and context-dependent. This is because identified mechanosensors (i.e., the receptors that become activated in response to flow) may not be functional in every type of vasculature, or for every developmental process. For instance, in zebrafish embryonic vessels, a mechanosensor that responds to hemodynamic force are non-motile cilia present on endothelial cells (Chen et al., 2017). However, analysis of non-motile cilia in mouse embryonic and extraembryonic (E8.5-E10.5) vessels, using a fluorescent reporter of non-motile cilia, revealed no primary cilia in mouse embryonic/extraembryonic vessels at E8.5-E10.5 (personal communication with Dr. Mary Dickinson). In another example, the glycocalyx participates in mechanotransduction under fluid shear stress to control endothelial cell behavior (Florian et al., 2003; Pahakis et al., 2007). During mouse embryonic development, the glycocalyx forms by embryonic day 10.0 (E10.0), and though it is required for vascular remodeling, impairment of glycocalyx formation does not block vSMC recruitment (Henderson-Toth et al., 2012). Pecam1/Vegfr2/Vecad have been shown to be a mechanosensory complex in endothelial cells that responds to shear stress by activating Akt (Tzima et al., 2005). However, our analysis comparing E9.5 reduced-flow and normal-flow yolk sac extracts revealed no difference in Akt activation (data not shown). Perhaps, this is due to the rapid activation of Akt observed in vitro (peaking at 1–5 min after shear stress)—time frames difficult to capture in vivo. Of course, these are just a few examples of identified mechanosensors in the endothelium. Thus, the roles of other mechanosensors (nuclei, ion channels, Integrins, caveolae, G-proteins, etc.) need to be further evaluated (Kutys and Chen, 2016). However, identifying relevant mechanosensory mechanisms may be very difficult to do because it is unclear the role that a single mechanosensor may play (perhaps a combinatorial effect is needed), and there may be time-sensitive responses to flow that are not captured by long-term responses to flow in vivo. Because of this complexity, we focused our analysis on mechanosensitive genes (which exhibit longer lasting changes in RNA expression) implicated in maturation.

Similar to the myriad of mechanotransduction mechanisms in the endothelium, there are also diverse ways to promote vSMC recruitment and coverage. Perhaps, the reason for this diversity relates to the varied origins of vSMC—differentiating from paraxial mesoderm, cardiac neural crest, proepicardium, secondary heart field, and mesothelial tissues (Majesky, 2007). Therefore, the mechanism(s) promoting coverage could be dependent on the context. Mechanisms could vary in arteries versus veins, in one vascularized organ versus another, or in blood vessels versus lymphatic vessels. As such, we analyzed whether expression of any vSMC recruitment/coverage genes was modulated by reduced-flow. Though we did not observe a change in *Angiopoietin 1*, *Pdgf-a/Pdgf-B*, *Netrin1*, and *EphrinB2/EphB4*, we did detect alterations in various *Sema3* genes, and in the Notch target gene *Hey1*. Regulation of expression of *Sema3* genes would be an interesting means of controlling vSMC recruitment, as Sema3 molecules are secreted. Thus, they could act as paracrine factors emanating from high-flow vessels to control vSMC recruitment over several cell distances. Interestingly, some of these Sema3 molecules have chemorepulsive and chemoattractive roles. So, it is possible that the observed upregulation Sema3a in reduced-flow, may highlight a potential role similar to lymphatic vessels, where it acts as a chemorepulsive molecule blocking vSMC recruitment to low-flow vessels (Jurisic et al., 2012). Whereas, the observed decrease of Sema3F and Sema3G in reduced-flow yolk sacs, may highlight a potential chemoattractant role for recruiting vSMCs to high-flow vessels. Chemoattractant roles for these Semaphorins have been documented as reexpression of Sema3F, in vivo, increases pericyte coverage (Wong et al., 2012), and expression of Sema3G induces gel migration of vSMCs, in vitro (Kutschera et al., 2011). More studies will need to be done to elucidate the roles of these combined Semaphorin 3 molecules in regulating vSMC recruitment in the embryo.

Though reduction of blood flow did not result in the downregulation of *Hey2*, it did result in the significant downregulation of *Hey1* (Fig. 5B). Interestingly, Hey1 and Hey2 are both required for the proper investment of vSMCs around many vessels in the embryo, and are both well-known Notch target genes (Fischer et al., 2004). Likewise, Notch signaling also has a well-known role in regulating vessel maturation (Benedito et al., 2009; High et al., 2008; Liu et al., 2009; Scheppke et al., 2012). The predominant mechanism of Notch during maturation involves signal-sending endothelial cells (i.e., the Delta and Jagged-expressing cells) communicating to juxtaposed signal-receiving vSMCs (i.e. the Notch-activated cells) to control vSMC coverage (Benedito et al., 2009; High et al., 2008; Liu et al., 2009; Scheppke et al., 2012). However, since we did not observe a downregulation in any of the Notch ligands in reduced-flow yolk sacs, we do not suspect this is the way in which *Hey1* is regulated by flow. Interestingly, reciprocal signaling has also been observed, whereby the vSMCs are the signal-sending cells and the endothelial cells are the signal-receiving cells, suggesting that Notch activation in the endothelium may also be important (Yang and Proweller, 2011). A role for Notch in the endothelium is of particular interest, as several in vitro and in vivo experiments have revealed that Notch receptor activity can be upregulated in the endothelium by shear stress/blood flow, and this regulation may occur through hemodynamic-force regulated mechanotransduction (Chen et al., 2017; Jahnsen et al., 2015; Masumura et al., 2009; Obi et al., 2009). The next obvious experiment would be to test for Notch activation in reduced-flow versus normal-flow vessels; however, we have not had success with Notch intracellular domain stainings. Thus, to provide further support for altered Notch signaling, we also looked at FoxC2 (and its paralogue FoxC1) which functions with the Notch intracellular domain to regulate Hey gene expression, and we observed a trend towards a downregulation in *FoxC2*, and a significant downregulation with *FoxC1*. Taken together, a possible model emerges whereby hemodynamic force promotes mechanotransduction in the endothelium leading to Notch activation. However, how activation of Notch in the endothelium contributes to adhesion to vSMCs remains unclear. More studies would need to be done to evaluate changes in cell adhesion molecules, or the extracellular matrix, that may regulate vSMC adhesion to the endothelium.

A potential outcome of our study is to have a better understanding of how people acquire blood vessel wall weaknesses caused by tunica media thinning. Thinning of the tunica media can arise in the embryo or fetus, such as in congenital aneurysm of the ascending aorta or a berry aneurysm. It can also arise in the adult, such as in segmental thinning of the umbilical cord, or even as an outcome of the aging process (Gupta et al., 2011). Though the cause of tunica media thinning could be due to various primary factors (genetic lesions or exposure to environmental agents), such factors could also affect blood flow patterns resulting in a secondary effect on vSMC coverage. For this reason, understanding both hemodynamic influences, as well as primary causes, will be important in developing therapies to prevent tunica media thinning. Thus, in future studies, further identifying and characterizing these mechanotransduction pathways controlling vSMC coverage may help to identify new therapeutic targets to counter problems with tunica media thinning.

Whether these therapeutic targets can be utilized to treat adult vessels remains to be determined. Encouragingly, vSMCs exhibit an interesting property that can be exploited. For instance, after terminal differentiation, many adult somatic cells remain quiescent, immobile and exhibit a specific functional characteristic. However, adult vSMCs have an ability to revert away from their contractile/functional form, lose adhesion, undergo proliferation and migrate to another region in the vasculature (Gomez and Owens, 2012). Thus, vSMCs can switch from a contractile state to a more malleable synthetic state, a process referred to as phenotypic modulation (Campbell and Campbell, 2012). Also, the recruitment and coverage of adult vSMCs have been highlighted in transplantation studies. When male patients received a heart transplant from a female donor, the new collateral coronary vessels that

grew become invested with vSMCs mostly originating from the male host (Quaini et al., 2002). Though the source of these vSMCs from the host was unclear (either from bone marrow-derived stem cells that differentiated into vSMCs, or from synthetic vSMCs), this study reveals the vSMCs are capable of being recruited to and covering adult vessels. Finally, it has been well studied that the very same molecules that promote proliferation and recruitment of vSMCs in the embryo, such as PdgfB, also play similar roles in the adult when overexpressed (Levanon et al., 2006). Taken together, this suggests that other types of relevant molecules that regulate vSMC recruitment and coverage, identified in this and other studies, could be utilized in a similar manner to repair vessels in the adult.

Supplementary data to this article can be found online at https://doi.org/10.1016/j.mod.2019.02.002.

Acknowledgements

Missouri State University's Office of Sponsored Research for animal care support.

Declarations of interest

None.

Funding

Missouri State University Graduate College funding (Rachel Padget), and Faculty Fellowship funding at Missouri State University (Ryan Udan).

References

Ambrus, J.L., Ambrus, C.M., Toumbis, C.A., Forgach, P., Karakousis, C.P., Niswander, P., Lane, W., 1991. Studies on tumor induced angiogenesis. J. Med. 22, 355–369.
Ando, K., Fukuhara, S., Izumi, N., Nakajima, H., Fukui, H., Kelsh, R.N., Mochizuki, N., 2016. Clarification of mural cell coverage of vascular endothelial cells by live imaging of zebrafish. Development 143, 1328–1339.
Armstrong, J.J., Larina, I.V., Dickinson, M.E., Zimmer, W.E., Hirschi, K.K., 2010. Characterization of bacterial artificial chromosome transgenic mice expressing mCherry fluorescent protein substituted for the murine smooth muscle α-actin gene. Genesis 48, 457–463.
Benedito, R., Roca, C., Sörensen, I., Adams, S., Gossler, A., Fruttiger, M., Adams, R.H., 2009. The notch ligands Dll4 and Jagged1 have opposing effects on angiogenesis. Cell 137, 1124–1135.
Blanco, R. and Gerhardt, H. (2013). VEGF and notch in tip and stalk cell selection. Cold Spring Harb. Perspect. Med. 3, a006569–a006569.
Cai, C.-L., Liang, X., Shi, Y., Chu, P.-H., Pfaff, S.L., Chen, J., Evans, S., 2003. Isl1 identifies a cardiac progenitor population that proliferates prior to differentiation and contributes a majority of cells to the heart. Dev. Cell 5, 877–889.
Campbell, J.H., Campbell, G.R., 2012. Smooth muscle phenotypic modulation—a personal experience. Arterioscler. Thromb. Vasc. Biol. 32, 1784–1789.
Chen, Q., Jiang, L., Li, C., Hu, D., Bu, J., Cai, D., Du, J., 2012. Haemodynamics-driven developmental pruning of brain vasculature in zebrafish. PLoS Biol. 10, e1001374.
Chen, X., Gays, D., Milia, C., Santoro, M.M., 2017. Cilia control vascular mural cell recruitment in vertebrates. Cell Rep. 18, 1033–1047.
Chong, D.C., Koo, Y., Xu, K., Fu, S., Cleaver, O., 2011. Stepwise arteriovenous fate acquisition during mammalian vasculogenesis. Dev. Dyn. 240, 2153–2165.
Culver, J.C., Dickinson, M.E., 2010. The effects of hemodynamic force on embryonic development. Microcirculation 17, 164–178.
Dewachter, L., Adnot, S., Fadel, E., Humbert, M., Maitre, B., Barlier-Mur, A.-M., Simonneau, G., Hamon, M., Naeije, R., Eddahibi, S., 2006. Angiopoietin/Tie2 pathway influences smooth muscle hyperplasia in idiopathic pulmonary hypertension. Am. J. Respir. Crit. Care Med. 174, 1025–1033.
Doi, H., Iso, T., Sato, H., Yamazaki, M., Matsui, H., Tanaka, T., Manabe, I., Arai, M., Nagai, R., Kurabayashi, M., 2006. Jagged1-selective notch signaling induces smooth muscle differentiation via a RBP-Jkappa-dependent pathway. J. Biol. Chem. 281, 28555–28564.
Domenga, V., Fardoux, P., Lacombe, P., Monet, M., Maciazek, J., Krebs, L. T., Klonjkowski, B., Berrou, E., Mericskay, M., Li, Z., et al. (2004). Notch3 is required for arterial identity and maturation of vascular smooth muscle cells. Genes Dev.. 18, 2730–2735.
Epstein, J.A., Aghajanian, H., Singh, M.K., 2015. Semaphorin signaling in cardiovascular development. Cell Metab. 21, 163–173.
Finney, A.C., Orr, A.W., 2018. Guidance molecules in vascular smooth muscle. Front. Physiol. 9, 1311.
Fischer, A., Schumacher, N., Maier, M., Sendtner, M., Gessler, M., 2004. The notch target genes Hey1 and Hey2 are required for embryonic vascular development. Genes Dev. 18, 901–911.
Florian, J.A., Kosky, J.R., Ainslie, K., Pang, Z., Dull, R.O., Tarbell, J.M., 2003. Heparan sulfate proteoglycan is a mechanosensor on endothelial cells. Circ. Res. 93, e136–e142.
Folkman, J., D'Amore, P.A., 1996. Blood vessel formation: what is its molecular basis? Cell 87, 1153–1155.
Foo, S.S., Turner, C.J., Adams, S., Compagni, A., Aubyn, D., Kogata, N., Lindblom, P., Shani, M., Zicha, D., Adams, R.H., 2006. Ephrin-B2 controls cell motility and adhesion during blood-vessel-wall assembly. Cell 124, 161–173.
French, W.J., Creemers, E.E., Tallquist, M.D., 2008. Platelet-derived growth factor receptors direct vascular development independent of vascular smooth muscle cell function. Mol. Cell. Biol. 28, 5646–5657.
Gale, N.W., Baluk, P., Pan, L., Kwan, M., Holash, J., DeChiara, T.M., McDonald, D.M., Yancopoulos, G.D., 2001. Ephrin-B2 selectively marks arterial vessels and neovascularization sites in the adult, with expression in both endothelial and smooth-muscle cells. Dev. Biol. 230, 151–160.
Garcia, M.D., Larina, I.V., 2014. Vascular development and hemodynamic force in the mouse yolk sac. Front. Physiol. 5, 308.
van Gils, J. M., Derby, M. C., Fernandes, L. R., Ramkhelawon, B., Ray, T. D., Rayner, K. J., Parathath, S., Distel, E., Feig, J. L., Alvarez-Leite, J. I. et al. (2012). The neuroimmune guidance cue netrin-1 promotes atherosclerosis by inhibiting the emigration of macrophages from plaques. Nat. Immunol. 13, 136–43.
Gomez, D., Owens, G.K., 2012. Smooth muscle cell phenotypic switching in atherosclerosis. Cardiovasc. Res. 95, 156–164.
Grotendorst, G.R., Chang, T., Seppä, H.E.J., Kleinman, H.K., Martin, G.R., 1982. Platelet-derived growth factor is a chemoattractant for vascular smooth muscle cells. J. Cell. Physiol. 113, 261–266.
Gu, C., Giraudo, E., 2013. The role of semaphorins and their receptors in vascular development and cancer. Exp. Cell Res. 319, 1306–1316.
Gupta, S.D., Gupta, S.K., Pal, D.K., Sarawagi, R., Gupta, P., 2011. Microscopic study of aorta in relation of different age groups: an observational study. Int. J. Biol. Med. Res. 2 (1), 398–403.
Hayashi, H., Kume, T., 2008. Foxc transcription factors directly regulate Dll4 and Hey2 expression by interacting with the VEGF-notch signaling pathways in endothelial cells. PLoS One 3, e2401.
Hellström, M., Kalén, M., Lindahl, P., Abramsson, A., Betsholtz, C., 1999. Role of PDGF-B and PDGFR-beta in recruitment of vascular smooth muscle cells and pericytes during embryonic blood vessel formation in the mouse. Development 126, 3047–3055.
Henderson-Toth, C.E., Jahnsen, E.D., Jamarani, R., Al-Roubaie, S., Jones, E.A.V., 2012. The glycocalyx is present as soon as blood flow is initiated and is required for normal vascular development. Dev. Biol. 369, 330–339.
High, F.A., Lu, M.M., Pear, W.S., Loomes, K.M., Kaestner, K.H., Epstein, J.A., 2008. Endothelial expression of the Notch ligand Jagged1 is required for vascular smooth muscle development. Proc. Natl. Acad. Sci. 105, 1955–1959.
Huang, C., Sheikh, F., Hollander, M., Cai, C., Becker, D., Chu, P.-H., Evans, S., Chen, J., 2003. Embryonic atrial function is essential for mouse embryogenesis, cardiac morphogenesis and angiogenesis. Development 130, 6111–6119.
Isayama, N., Matsumura, G., Yamazaki, K., 2013. Comparison of vascular smooth muscle cells in canine great vessels. BMC Vet. Res. 9, 54.
Jahnsen, E.D., Trindade, A., Zaun, H.C., Lehoux, S., Duarte, A., Jones, E.A.V., 2015. Notch1 is pan-endothelial at the onset of flow and regulated by flow. PLoS One 10, e0122622.
Jawien, A., Bowen-Pope, D.F., Lindner, V., Schwartz, S.M., Clowes, A.W., 1992. Platelet-derived growth factor promotes smooth muscle migration and intimal thickening in a rat model of balloon angioplasty. J. Clin. Invest. 89, 507–511.
Jones, E.A.V., Yuan, L., Breant, C., Watts, R.J., Eichmann, A., 2008. Separating genetic and hemodynamic defects in neuropilin 1 knockout embryos. Development 135, 2479–2488.
Jurisic, G., Maby-El Hajjami, H., Karaman, S., Ochsenbein, A.M., Alitalo, A., Siddiqui, S.S., Ochoa Pereira, C., Petrova, T.V., Detmar, M., 2012. An unexpected role of Semaphorin3A–Neuropilin-1 signaling in lymphatic vessel maturation and valve formation. Circ. Res. 111, 426–436.
Korff, T., Braun, J., Pfaff, D., Augustin, H.G., Hecker, M., 2008. Role of ephrinB2 expression in endothelial cells during arteriogenesis: impact on smooth muscle cell migration and monocyte recruitment. Blood 112, 73–81.
Kutschera, S., Weber, H., Weick, A., De Smet, F., Genove, G., Takemoto, M., Prahst, C., Riedel, M., Mikelis, C., Baulande, S., et al. (2011). Differential endothelial transcriptomics identifies Semaphorin 3G as a vascular class 3 Semaphorin. Arterioscler. Thromb. Vasc. Biol. 31, 151–159.
Kutys, M.L., Chen, C.S., 2016. Forces and mechanotransduction in 3D vascular biology. Curr. Opin. Cell Biol. 42, 73–79.
Levanon, K., Varda-Bloom, N., Greenberger, S., Barshack, I., Goldberg, I., Orenstein, A., Breitbart, E., Shaish, A., Harats, D., 2006. Vascular wall maturation and prolonged angiogenic effect by endothelial-specific platelet-derived growth factor expression. Pathobiology 73, 149–158.
Lindahl, P., Johansson, B.R., Levéen, P., Betsholtz, C., 1997. Pericyte loss and microaneurysm formation in PDGF-B-deficient mice. Science 277, 242–245.
Liu, H., Kennard, S., Lilly, B., 2009. NOTCH3 expression is induced in mural cells through an autoregulatory loop that requires endothelial-expressed JAGGED1. Circ. Res. 104, 466–475.
Livak, K.J., Schmittgen, T.D., 2001. Analysis of relative gene expression data using real-time quantitative PCR and the $2-\Delta\Delta CT$ method. Methods 25, 402–408.
Lucitti, J.L., Jones, E.A.V., Huang, C., Chen, J., Fraser, S.E., Dickinson, M.E., 2007. Vascular remodeling of the mouse yolk sac requires hemodynamic force. Development 134, 3317–3326.

Mack, C.P., 2011. Signaling mechanisms that regulate smooth muscle cell differentiation. Arterioscler. Thromb. Vasc. Biol. 31, 1495–1505.
Majesky, M.W., 2007. Developmental Basis of Vascular Smooth Muscle Diversity.
Masumura, T., Yamamoto, K., Shimizu, N., Obi, S., Ando, J., 2009. Shear stress increases expression of the arterial endothelial marker EphrinB2 in murine ES cells via the VEGF-notch signaling pathways. Arterioscler. Thromb. Vasc. Biol. 29, 2125–2131.
le Noble, F., Moyon, D., Pardanaud, L., Yuan, L., Djonov, V., Matthijsen, R., Bréant, C., Fleury, V., Eichmann, A., 2003. Flow regulates arterial-venous differentiation in the chick embryo yolk sac. Development 131, 361–375.
Obi, S., Yamamoto, K., Shimizu, N., Kumagaya, S., Masumura, T., Sokabe, T., Asahara, T., Ando, J., 2009. Fluid shear stress induces arterial differentiation of endothelial progenitor cells. J. Appl. Physiol. 106, 203–211.
Pahakis, M.Y., Kosky, J.R., Dull, R.O., Tarbell, J.M., 2007. The role of endothelial glycocalyx components in mechanotransduction of fluid shear stress. Biochem. Biophys. Res. Commun. 355, 228–233.
Quaini, F., Urbanek, K., Beltrami, A.P., Finato, N., Beltrami, C.A., Nadal-Ginard, B., Kajstura, J., Leri, A., Anversa, P., 2002. Chimerism of the transplanted heart. N. Engl. J. Med. 346, 5–15.
Ross, R., Glomset, J., Kariya, B., Harker, L., 1974. A platelet-dependent serum factor that stimulates the proliferation of arterial smooth muscle cells in vitro. Proc. Natl. Acad. Sci. U. S. A. 71, 1207–1210.
Ruiz-Lozano, P., Smith, S.M., Perkins, G., Kubalak, S.W., Boss, G.R., Sucov, H.M., Evans, R.M., Chien, K.R., 1998. Energy deprivation and a deficiency in downstream metabolic target genes during the onset of embryonic heart failure in RXRalpha−/− embryos. Development 125, 533–544.
Scheppke, L., Murphy, E. A., Zarpellon, A., Hofmann, J. J., Merkulova, A., Shields, D. J., Weis, S. M., Byzova, T.V., Ruggeri, Z. M., Iruela-Arispe, M. L. et al. (2012). Notch promotes vascular maturation by inducing integrin-mediated smooth muscle cell adhesion to the endothelial basement membrane. Blood 119, 2149–58.
Shin, D., Garcia-Cardena, G., Hayashi, S.-I., Gerety, S., Asahara, T., Stavrakis, G., Isner, J., Folkman, J., Gimbrone, M.A., Anderson, D.J., 2001. Expression of EphrinB2 identifies a stable genetic difference between arterial and venous vascular smooth muscle as well as endothelial cells, and marks subsets of microvessels at sites of adult neovascularization. Dev. Biol. 230, 139–150.
Suri, C., Jones, P.F., Patan, S., Bartunkova, S., Maisonpierre, P.C., Davis, S., Sato, T.N., Yancopoulos, G.D., 1996. Requisite role of angiopoietin-1, a ligand for the TIE2 receptor, during embryonic angiogenesis. Cell 87, 1171–1180.
Tzima, E., Irani-Tehrani, M., Kiosses, W.B., Dejana, E., Schultz, D.A., Engelhardt, B., Cao, G., DeLisser, H., Schwartz, M.A., 2005. A mechanosensory complex that mediates the endothelial cell response to fluid shear stress. Nature 437, 426–431.
Udan, R.S., Culver, J.C., Dickinson, M.E., 2013a. Understanding vascular development. Wiley Interdiscip. Rev. Dev. Biol. 2.
Udan, R.S., Vadakkan, T.J., Dickinson, M.E., 2013b. Dynamic responses of endothelial cells to changes in blood flow during vascular remodeling of the mouse yolk sac. Dev 140.
Vikkula, M., Boon, L. M., Carraway, K. L., Calvert, J. T., Diamonti, A. J., Goumnerov, B., Pasyk, K. A., Marchuk, D. A., Warman, M. L., Cantley, L. C. et al. (1996). Vascular dysmorphogenesis caused by an activating mutation in the receptor tyrosine kinase TIE2. Cell 87, 1181–90.
Wang, H.U., Chen, Z.F., Anderson, D.J., 1998. Molecular distinction and angiogenic interaction between embryonic arteries and veins revealed by ephrin-B2 and its receptor Eph-B4. Cell 93, 741–753.
Wilting, J., Christ, B., Bokeloh, M., Weich, H.A., 1993. In vivo effects of vascular endothelial growth factor on the chicken chorioallantoic membrane. Cell Tissue Res. 274, 163–172.
Wong, H.-K., Shimizu, A., Kirkpatrick, N.D., Garkavtsev, I., Chan, A.W., di Tomaso, E., Klagsbrun, M., Jain, R.K., 2012. Merlin/NF2 regulates angiogenesis in schwannomas through a Rac1/semaphorin 3F-dependent mechanism. Neoplasia 14, 84–94.
Yang, K., Proweller, A., 2011. Vascular smooth muscle notch signals regulate endothelial cell sensitivity to angiogenic stimulation. J. Biol. Chem. 286, 13741–13753.
Yashiro, K., Shiratori, H., Hamada, H., 2007. Haemodynamics determined by a genetic programme govern asymmetric development of the aortic arch. Nature 450, 285–288.